**Steel and Composite Structures**, *Vol. 19, No. 2 (2015) 485-501*
DOI: http://dx.doi.org/10.12989/scs.2015.19.2.485 

# Analytical study of composite beams with different arrangements of channel shear connectors

Nader Fanaie [1a], Farzaneh Ghalamzan Esfahani [*1] and Soheil Soroushnia [2b]

[1] *Department of Civil Engineering, K. N. Toosi University of Technology, Tehran, Iran*
[2] *Islamic Azad University, Takestan Branch, Takestan, Iran*

(*Received April 26, 2014, Revised April 22, 2015, Accepted May 13, 2015*)

**Abstract.** Channels are implemented in composite beams as shear connectors in two arrangements, face to face and back to back. No relevant explanation is found in the design codes to clarify the preference of the mentioned arrangements. Besides, the designers do not have a common opinion on this subject; i.e., some recommend the face to face and others, back to back status. In this research, channel shear connectors in composite beams are studied analytically for both arrangements using ABAQUS software. For this purpose, they have been modeled in simply supported beams in the arrangements of face to face and back to back; their effects on the crack initiation load of concrete slabs were monitored. The stiffness values of composite beams were also compared in the two arrangements using force-displacement curve; the results are relatively the same in both cases. Furthermore, the effects of compressive strength of concrete, channel size, length and spacing of channels as well as steel type of channels on the performance of composite beams have been investigated. According to the results obtained in this research, the face to face status shows better performance in comparison with that of back to back, considering the load of concrete fracturing.

**Keywords:** composite beam; channel shear connector; face to face; back to back; crack

## 1. Introduction

Nowadays, composite beams are widely implemented in bridges and ordinary buildings in developed countries and considered as the appropriate solution to cover spans of medium lengths (Salmon and Johnson 1996). Numerous scientific documents have been published by researchers since the development and construction of composite beams (Brendel 1964, Viest 1974, Nguyen *et al*. 2009, Chung and Chan 2011). Besides transferring the shear existing between steel beams and concrete slabs, shear connectors play important roles in conserving the integrity of concrete slabs with the beam section, preventing it from moving up the steel beam (Pashan 2006). In order to obtain proper performance in the composite beam, shear connectors should have enough stiffness to prevent sliding at the connection point. Although stud shear connectors are the most common ones, some other older types such as channels and T-shape sections are still in use (Abe and

*Corresponding author, M.Sc. in Structural Engineering, E-mail: f.ghalamzan@gmail.com
[a] Ph.D., E-mail: fanaie@kntu.ac.ir
[b] M.Sc. in Structural Engineering, E-mail: soroushnia@gmail.com


http://www.techno-press.org/?journal=scs&subpage=8 ISSN: 1229-9367 (Print), 1598-6233 (Online)

Hosaka 2002). Recent researches have studied the load–displacement behavior and the shear capacity of channel shear connectors in composite beams from the experimental and analytical push-out or beam tests (Maleki and Mahoutian 2009, Shariati *et al*. 2012). The channel connectors do not require special equipment; standard welding procedures are adequate for attachment purposes (Baran and Topkaya 2012). In addition, this type of connector showed more shear strength than angle shear connectors (Shariati *et al*. 2013).

When channels are used as shear connectors, they should be laid out in such a way that the channel has enough confinement in the concrete. The channels are implemented in two arrangements of face to face and back to back. There is no relevant explanation in AISC code (AISC 2010) to clarify the preference of the mentioned arrangements. Besides, the experts and designers have no consensus on this subject; i.e., some recommend the face to face and some others, back to back status. In this research, the effect of channel shear connectors on the performance of composite beams is studied through exact modeling of finite element by ABAQUS software (Hibbitt *et al*. 2011) by changing the compressive strength of concrete, channel size, length and spacing of channels and steel grade of channel.

## 2. Finite element model

ABAQUS finite element software was used for conducting numerical analyses through C3D8R elements, eight-node linear hexahedral solid elements with reduced integration, as shown in Fig. 1. The IPE270 with 270 mm height, flange width of 135 mm, web thickness of 6.6 mm and flange thickness of 10.2 mm were used as steel profile in the modeling. The concrete slab has a thickness of 150 mm and an effective width of 600 mm (Fig. 2). The beam length was considered as 4.5 m. The type of contact between the concrete slab and the steel profile is general with the specifications of tangential behavior with friction coefficient of 0.25. Normal behaviors are of hard contact types. This contact prevents the penetration of concrete slab into the beam section. Furthermore, the separation after contact of the concrete slab and the steel beam was allowed in all of the models.

### *2.1 Boundary conditions*

The beam was considered as simply supported. The lateral supports were located based on the appropriate spacing in order to prevent out of plane movement of the beam web as well as the lateral torsional buckling of the steel beam. The loading type and supports are shown in Fig. 3. Load control analysis was used in this study.

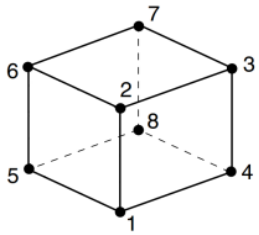


Fig. 1 8-node linear hexahedral solid element with reduced integration (C3D8R)

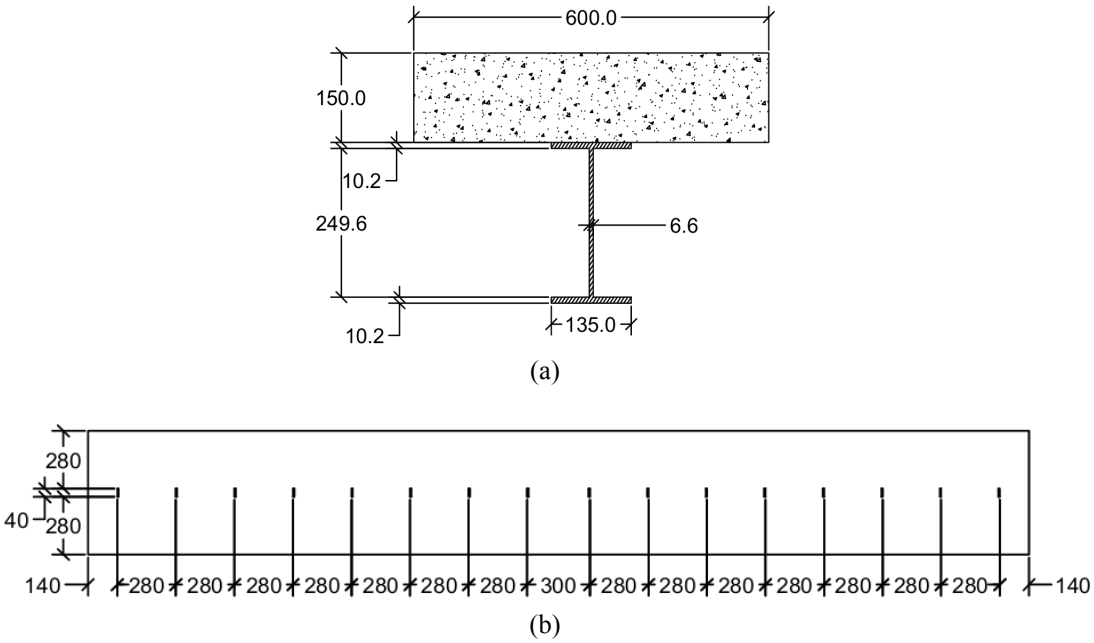


Fig. 2 (a) Composite beam cross-section (dimensions in mm); (b) slab plan and channel shear connectors with 40 mm length

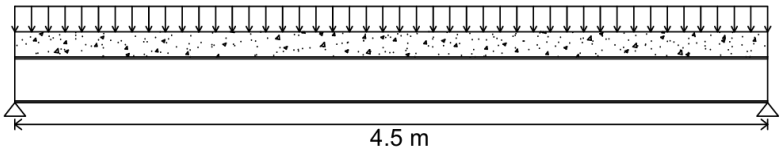


Fig. 3 Supports and loading type

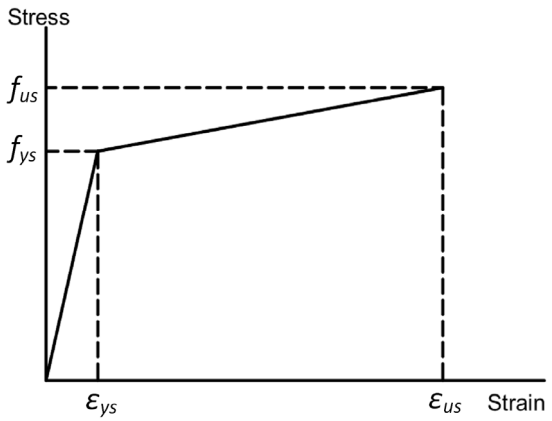


Fig. 4 Stress-strain diagram of the steel

### 2.2 The specifications of the materials

#### 2.2.1 Steel

The behavior of steel was considered as elastic-plastic in order to model the nonlinear behavior of the steel. The stress-strain curve of steel was plotted for compression and tension as shown in Fig. 4. The steel had elastic behavior with an elasticity modulus of $E_s$ up to yielding stress ($f_{ys}$). It then arrived at the plastic range with a slight slope up to ultimate stress ($f_{us}$) and ultimate strain ($\varepsilon_{us}$).

The applied steel types are ST37 and ST52. ST37 has a yielding stress of 240 MPa and an ultimate stress of 360 MPa. The elasticity modulus and ultimate strain of steel are assumed as 200 GPa and 20% respectively. Considering these quantities, the plastic stiffness (slope of stress-strain diagram in plastic region) is calculated as 604 MPa, which is about $0.003E_s$. The stress-strain curve upon reaching $f_{us}$ is assumed to be horizontal with no stiffness (elastic-perfectly plastic model) (Maleki and Bagheri 2008a, b). ST52 has a yielding stress of 359 MPa and an ultimate stress of 510 MPa. Its elasticity modulus and ultimate strain was considered as 200 GPa and 25% respectively (Vasdravellis *et al*. 2012). Beam section material is ST37 in all of the models and the steel type of channels are changed to ST37 and ST52 according to Table 4.

#### 2.2.2 Concrete

Fig. 5 shows the stress-strain diagram used for the concrete. The initial slope of the curve in the compression region is $E_{ci}$, which is the modulus of elasticity for 28 day concrete (Code 1990).

Maximum compressive strength of concrete can be presented as follows

$$f_{cm} = f_{ck} + \Delta f, \quad \Delta f = 8\,\text{MPa} \tag{1}$$

Where $f_{ck}$ is the characteristic strength of cylindrical sample of 28 day concrete.

Secant modulus of elasticity can be presented versus tangential modulus of elasticity as follows

$$E_{ci} = E_{co}\left[\frac{f_{cm}}{f_{cmo}}\right]^{\frac{1}{3}} \tag{2}$$

$$f_{cmo} = 10\,\text{MPa} \tag{3}$$

$$E_{co} = 2.15\times10^4\ \text{MPa} \tag{4}$$

Stress of concrete can be calculated using the following formulas

$$\sigma_c = -\frac{\dfrac{E_{ci}\varepsilon_c}{E_{c1}\varepsilon_{c1}} - \left(\dfrac{\varepsilon_c}{\varepsilon_{c1}}\right)^2}{1+\left(\dfrac{E_{ci}}{E_{c1}}-2\right)\dfrac{\varepsilon_c}{\varepsilon_{c1}}} f_{cm} \qquad |\varepsilon_c| < |\varepsilon_{c,\text{lim}}| \tag{5}$$

$$\varepsilon_{c1} = -0.0022 \tag{6}$$

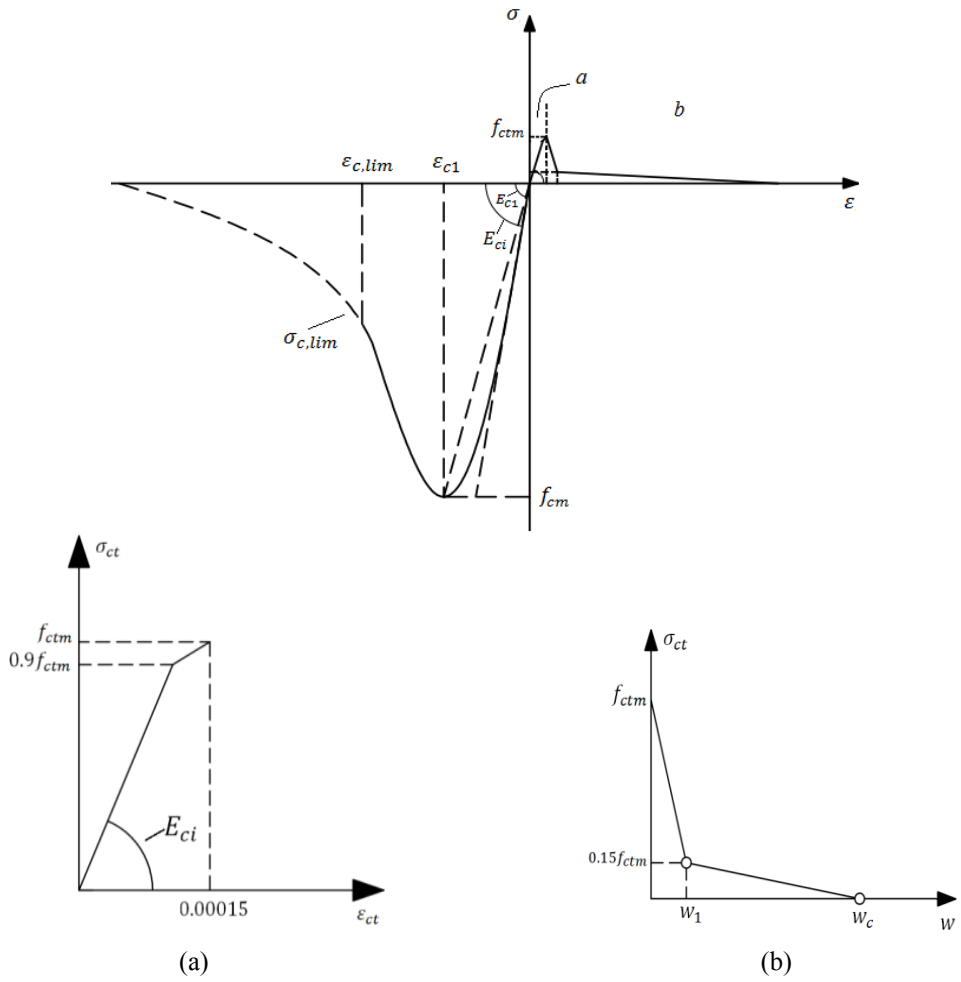


(a) (b)

Fig. 5 The stress-strain diagram of concrete: (a) stress-strain diagram in the tension status before crack formation; (b) stress-strain diagram in the tension status after crack formation

$$E_{c1} = \frac{f_{cm}}{0.0022} \tag{7}$$

$$\frac{\varepsilon_{c,\lim}}{\varepsilon_{c1}} = \frac{1}{2}\left(\frac{1}{2}\frac{E_{ci}}{E_{c1}} + 1\right) + \left[\frac{1}{4}\left(\frac{1}{2}\frac{E_{ci}}{E_{c1}} + 1\right)^2 - \frac{1}{2}\right]^{1/2} \tag{8}$$

Where $\varepsilon_{c,\lim}$ is the strain corresponding to $\sigma_{c,\lim} = -0.5f_{cm}$. The stress-strain diagram has been plotted for the concrete in the case of tension loading and shown in Figs. 5(a) and (b). In tension, the curve remains linear with $E_{ci}$ slope until arriving at the $0.9f_{ctm}$ stress value as shown in Fig. 5(a). $f_{ctm}$ is the tension strength of the concrete which is obtained from Eq. (9). The stress-strain diagram is obtained by Eq. (12) for the stress values of $0.9f_{ctm}$ to $f_{ctm}$. When the stress value gets to $f_{ctm}$, after crack formation, the stress-strain diagram is shown in Fig. 5(b).

$$f_{ctm} = f_{ctko,m}\left(\frac{f_{ck}}{f_{cko}}\right)^{\frac{2}{3}} \tag{9}$$

$$f_{ctko,m} = 1.4 \text{ MPa} \tag{10}$$

$$f_{cko} = 10 \text{ MPa} \tag{11}$$

$$\sigma_{ct} = f_{ctm} - \frac{0.1 f_{ctm}}{0.00015 - 0.9\frac{f_{ctm}}{E_{ci}}}\left(0.00015 - \varepsilon_{ct}\right) \qquad 0.9 f_{ctm} < \sigma_{ct} \le f_{ctm} \tag{12}$$

If the stress is between $0.15f_{ctm}$ and $f_{ctm}$, then the stress-strain diagram is obtained from Eq. (13). By increasing the crack size and by arriving at a stress value of $0.15f_{ctm}$, the slope of the curve is changed and the diagram is obtained by Eq. (14) (Code 1990).

Stress-strain diagram after crack formation in the case of tension loading (corresponding to Fig. 5(b)) can be calculated as follows

$$\sigma_{ct} = f_{ctm}\left(1 - 0.85\frac{w}{w_1}\right) \qquad 0.15 f_{ctm} \le \sigma_{ct} < f_{ctm} \tag{13}$$

$$\sigma_{ct} = \frac{0.15 f_{ctm}}{w_c - w_1}\left(w_c - w\right) \qquad 0 \le \sigma_{ct} < 0.15 f_{ctm} \tag{14}$$

$$w_1 = 2\frac{G_F}{f_{ctm}} - 0.15 w_c \tag{15}$$

$$w_c = \alpha_F \frac{G_F}{f_{ctm}} \tag{16}$$

Where, $w_1$ is the crack size when $\sigma_{ct} = 0.15f_{ctm}$; $w_c$ is the crack size when $\sigma_{ct} = 0$; $\alpha_F$ is a coefficient related to the maximum size of concrete aggregate obtained from Table 1; $G_F$ is the fracture energy needed for propagating a tension crack in the unit area. The maximum size of the concrete aggregate was considered as 8 mm in the conducted numerical models (Code 1990). If no experimental information exists, then the fracture energy is obtained from the formula below

$$G_F = G_{F0}\left(\frac{f_{cm}}{f_{cmo}}\right)^{0.7} \tag{17}$$

The value of $G_{F0}$ is the fracture energy base which is related to the maximum size of the concrete aggregate and obtained from Table 2.

The concrete samples with compressive strengths of 25, 30 and 35 MPa were used in this research to study the effect of compressive strength on the performance of channel shear connectors. The stress-strain diagrams for these concrete samples are shown in Figs. 6 to 8.

Table 1 Applied coefficient in the Eq. (16) for estimating $w_c$

| $d_{max}$ (mm) | 8 | 16 | 32 |
|---|---|---|---|
| $\alpha_F$ | 8 | 7 | 5 |

Table 2 Base values of fracture energy ($G_{F0}$) versus maximum size of concrete aggregate

| $d_{max}$ (mm) | $G_{F0}$ (N.mm/mm$^2$) |
|---|---|
| 8 | 0.025 |
| 16 | 0.03 |
| 32 | 0.058 |

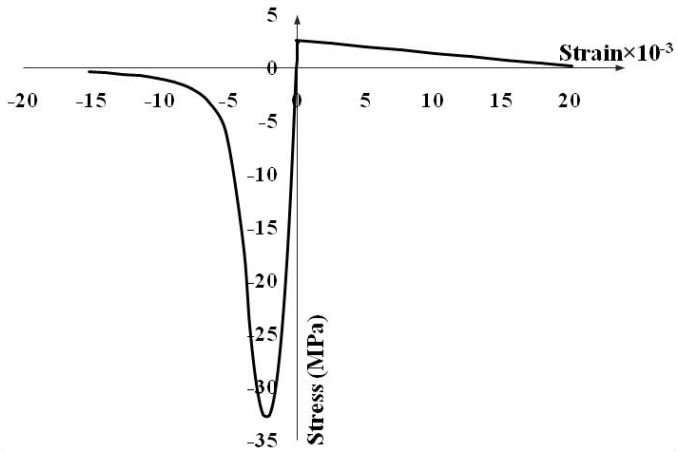


Fig. 6 Stress-strain diagram of concrete with the compressive strength of 25 MPa

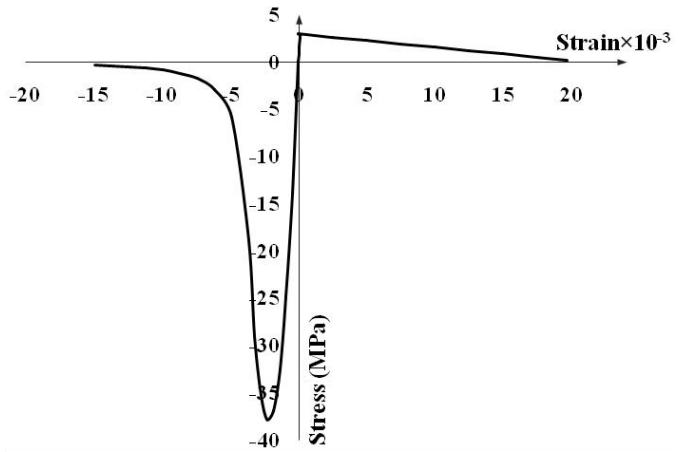


Fig. 7 Stress-strain diagram of concrete with the compressive strength of 30 MPa

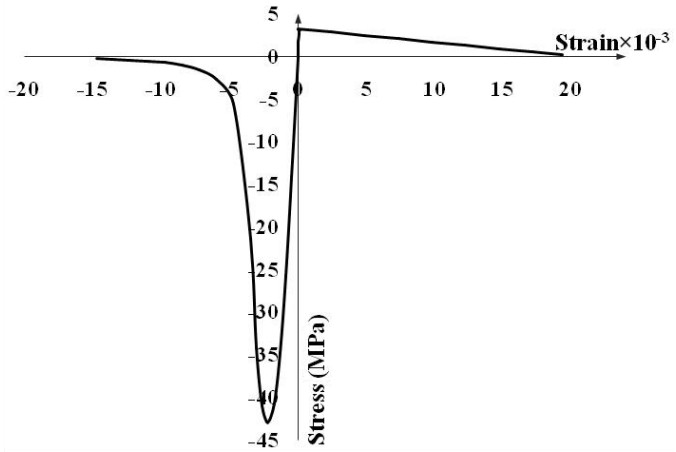


Fig. 8 Stress-strain diagram of concrete with the compressive strength of 35 MPa

Table 3 Geometric properties of channels

| Channel | $h\,(mm)$ | $t_w\,(mm)$ | $b\,(mm)$ | $t_f\,(mm)$ |
|---|---|---|---|---|
| UNP60 | 60 | 6 | 30 | 6 |
| UNP80 | 80 | 6 | 45 | 8 |
| UNP100 | 100 | 6 | 50 | 8.5 |

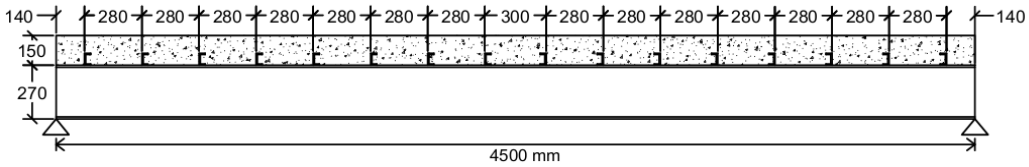


(a) Face to face

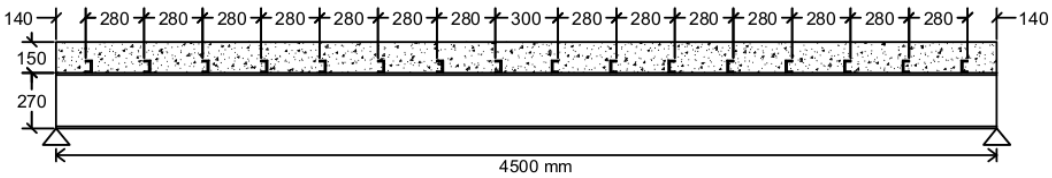


(b) Back to back

Fig. 9 The locations of 16 channels

UNP60, 80 and 100 were used for channel shear connectors in order to study the effect of channel size on the performance of composite beam. The geometric properties of the channels are shown in Table 3. The channel steel type is shown in Table 4.

To study the effects of length and spacing of channel shear connectors on force-displacement diagram and crack initiation load, 16 UNP60 of 4 cm length and 28 cm spacing, 16 UNP60 of

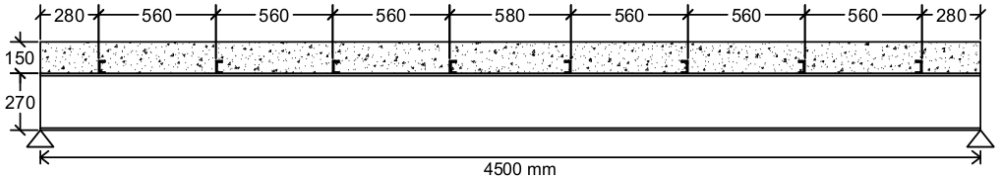


(a) Face to face

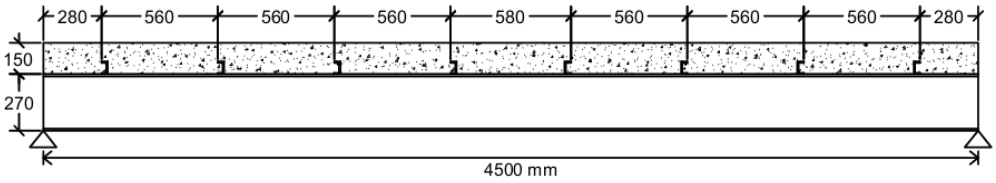


(b) Back to back

Fig. 10 The locations of 8 channels

Table 4 Specifications of the models

| Model | Channel height(mm) | Channel length(mm) | $f_c$ (MPa) | Number of channels | Channel steel type | Position |
|---|---|---|---|---|---|---|
| C60-40-25-16-f | 60 | 40 | 25 | 16 | ST37 | face to face |
| C60-40-30-16-f | 60 | 40 | 30 | 16 | ST37 | face to face |
| C60-40-35-16-f | 60 | 40 | 35 | 16 | ST37 | face to face |
| C60-80-25-16-f | 60 | 80 | 25 | 16 | ST37 | face to face |
| C60-80-30-16-f | 60 | 80 | 30 | 16 | ST37 | face to face |
| C60-80-35-16-f | 60 | 80 | 35 | 16 | ST37 | face to face |
| C60-80-25-8-f | 60 | 80 | 25 | 8 | ST37 | face to face |
| C60-80-30-8-f | 60 | 80 | 30 | 8 | ST37 | face to face |
| C60-80-35-8-f | 60 | 80 | 35 | 8 | ST37 | face to face |
| C80-40-25-16-f | 80 | 40 | 25 | 16 | ST37 | face to face |
| C80-40-30-16-f | 80 | 40 | 30 | 16 | ST37 | face to face |
| C80-40-35-16-f | 80 | 40 | 35 | 16 | ST37 | face to face |
| C100-40-25-16-f | 100 | 40 | 25 | 16 | ST37 | face to face |
| C100-40-30-16-f | 100 | 40 | 30 | 16 | ST37 | face to face |
| C100-40-35-16-f | 100 | 40 | 35 | 16 | ST37 | face to face |
| C60-40-25-16-b | 60 | 40 | 25 | 16 | ST37 | back to back |
| C60-40-30-16-b | 60 | 40 | 30 | 16 | ST37 | back to back |
| C60-40-35-16-b | 60 | 40 | 35 | 16 | ST37 | back to back |
| C60-80-25-16-b | 60 | 80 | 25 | 16 | ST37 | back to back |
| C60-80-30-16-b | 60 | 80 | 30 | 16 | ST37 | back to back |
| C60-80-35-16-b | 60 | 80 | 35 | 16 | ST37 | back to back |
| C60-80-25-8-b | 60 | 80 | 25 | 8 | ST37 | back to back |

Table 4 Continued

| Model | Channel height(mm) | Channel length(mm) | $f_c$ (MPa) | Number of channels | Channel steel type | Position |
|---|---|---|---|---|---|---|
| C60-80-30-8-b | 60 | 80 | 30 | 8 | ST37 | back to back |
| C60-80-35-8-b | 60 | 80 | 35 | 8 | ST37 | back to back |
| C80-40-25-16-b | 80 | 40 | 25 | 16 | ST37 | back to back |
| C80-40-30-16-b | 80 | 40 | 30 | 16 | ST37 | back to back |
| C80-40-35-16-b | 80 | 40 | 35 | 16 | ST37 | back to back |
| C100-40-25-16-b | 100 | 40 | 25 | 16 | ST37 | back to back |
| C100-40-30-16-b | 100 | 40 | 30 | 16 | ST37 | back to back |
| C100-40-35-16-b | 100 | 40 | 35 | 16 | ST37 | back to back |
| C60-40-25-16-f-ST52 | 60 | 40 | 25 | 16 | ST52 | face to face |
| C60-40-25-16-b-ST52 | 60 | 40 | 25 | 16 | ST52 | back to back |

8 cm length and 28 cm spacing, and 8 UNP60 of 8 cm length and 56 cm spacing were considered for the channel shear connectors. The situations of 16 and 8 channels are shown in Figs. 9 and 10 respectively, in both cases of face to face and back to back. The crack initiation load is the distributed load applied to the beam on which the first cracking symptoms are found. The crack is initiated at the points where the plastic strain value of the concrete is higher than zero (Lubliner *et al*. 1989). Considering the analyzed specimens, the first symptoms of plastic strain are formed at the contact surface of concrete to the steel beam. The points of crack initiation load are presented in Figs. 12 to 21. These points are obtained by monitoring the concrete parts of the specimens, considering the time of plastic strain formed at the surface of concrete in contact with the steel beam and they are shown on the force-displacement diagrams of composite beams.

Two kinds of steel, ST37 and ST52 were used for the channels of UNP60 with 4 cm length in order to study the effect of steel grade on the performance of channel shear connectors. The results have been derived for both arrangements of face to face and back to back presented in Section 3.5. The specifications of considered models have been summarized in Table 4. In the first column of Table 4, the letters “f” and “b” represent “face to face” and “back to back” situations respectively.

## 3. The results of software analysis

### *3.1 Verification*

In order to verify the validity of the finite element model, the specimen with 4 channel shear connectors used in the experimental study conducted by Baran and Topkaya (2014) was analyzed under monotonic loading using ABAQUS finite element software. Moment-deflection diagram of the model is shown in Fig. 11. According to Fig. 11, the results are in agreement with the experimental results.

### *3.2 The effect of compressive strength of concrete*

Force-displacement diagrams of composite beam were plotted with regards to face to face and back to back arrangements of the channels UNP60, 80 and 100 of 4 cm length for concrete with

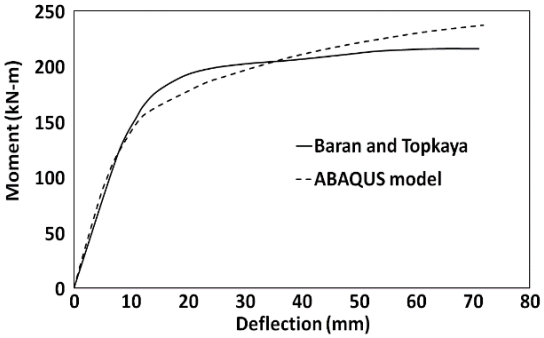


Fig. 11 Moment- deflection diagram of model for verification

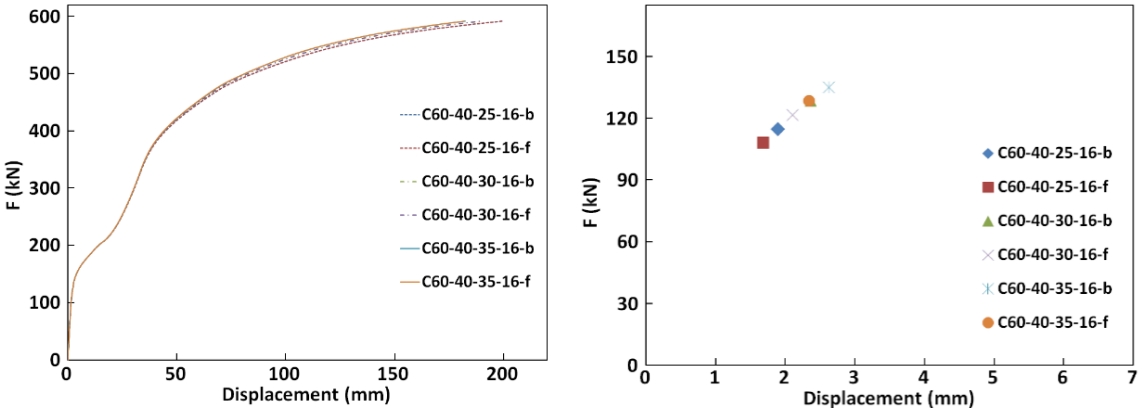


(a) Force-displacement diagram (b) Crack initiation load point

Fig. 12 Composite beams with different compressive strengths (UNP60)

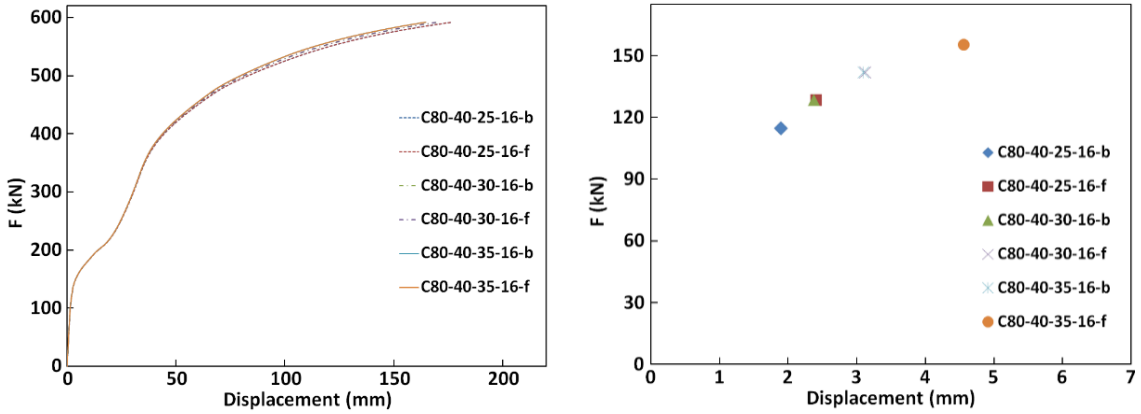


(a) Force-displacement diagram (b) Crack initiation load point

Fig. 13 Composite beams with different compressive strengths (UNP80)

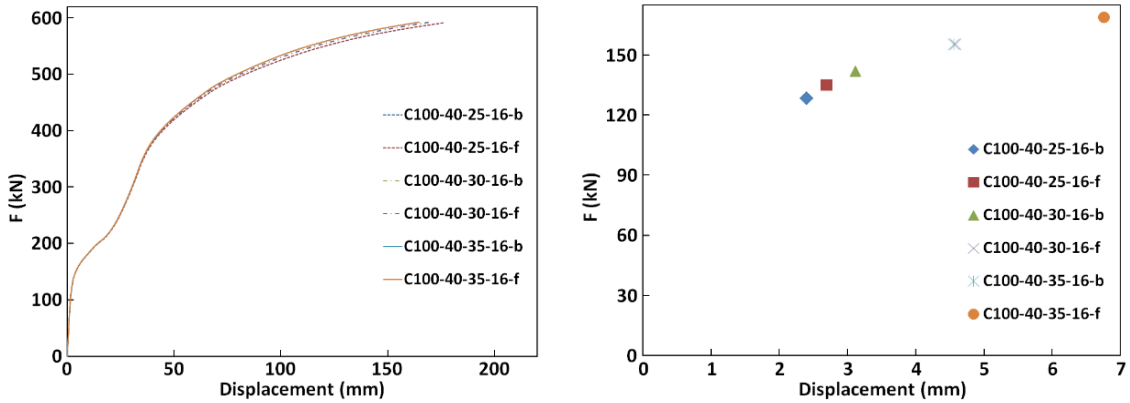


(a) Force-displacement diagram (b) Crack initiation load point

Fig. 14 Composite beams with different compressive strengths (UNP100)

compressive strengths of 25, 30 and 35 MPa and shown in Figs. 12 to 14. In these plots, vertical axis is total reaction forces and horizontal axis is central displacement of the beam.

Based on the figures, if the compressive strength of concrete barely increases, final displacement is also slightly changed and the results coincide in both arrangements (face to face and back to back).

The crack initiation load rises with increasing compressive strength in all of the specimens with different channel sizes. According to Fig. 12(b), plotted for the specimen with UNP60, the cracking time of concrete is slightly more in back to back arrangement in all of the specimens compared to that of face to face arrangement. However, the crack is formed later in the face to face status in the concrete of the specimens with UNP80 and UNP100 channels for different compressive strengths in comparison to that of back to back. It means that more forces are needed for the formation of plastic strain in the concrete. Based on Figs. 12 to 14, the effect of compressive strength of concrete is higher at the crack initiation load points for composite beams with UNP80 and UNP100 compared to that with UNP60.

### *3.3 The effect of channel size*

Force-displacement diagram of composite beam was plotted for two arrangements of face to face and back to back of UNP60, UNP80 and UNP100 channels with length of 4 cm and presented for the concrete with compressive strengths of 25, 30 and 35 MPa.

As shown in Figs. 15 to 17, for a constant compressive strength of concrete and for large amount of loadings, the displacement decreases when the channel size increases from UNP60 to UNP80. However, no significant difference is seen in the results when channel size increases from UNP80 to UNP100. The results are the same in all models for both arrangements of face to face and back to back.

The crack initiation load rises with increasing size of channel; it means that the concrete was fractured later. According to Fig. 15(b), presented for specimens with 25 MPa compressive strength, the crack initiation load rises slightly with increasing size of channel. However, based on Figs. 16(b) and 17(b), presented for specimens with 30 and 35 MPa compressive strengths, the

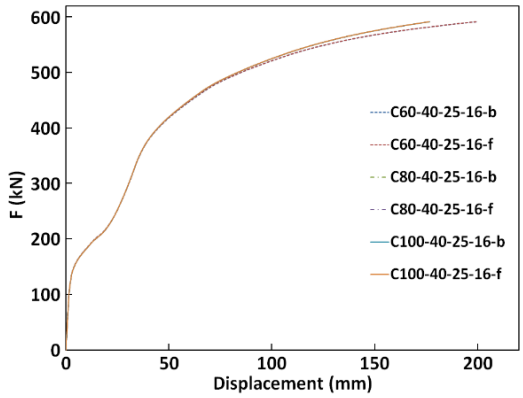


(a) Force-displacement diagram

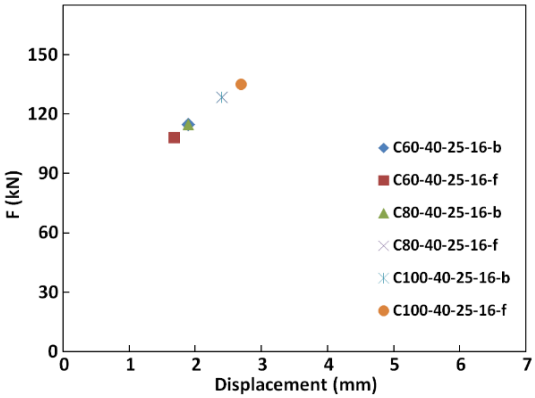


(b) Crack initiation load point

Fig. 15 Composite beam with different channels in face to face and back to back arrangements ($f_c$ = 25 MPa)

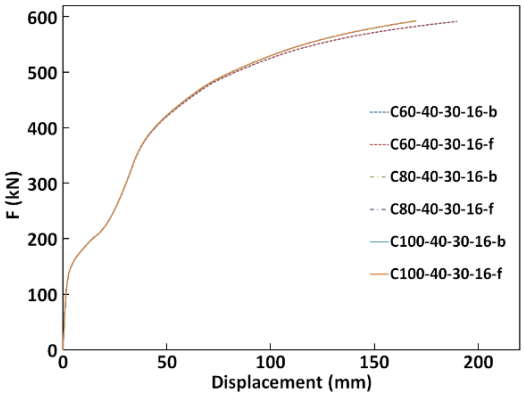


(a) Force-displacement diagram

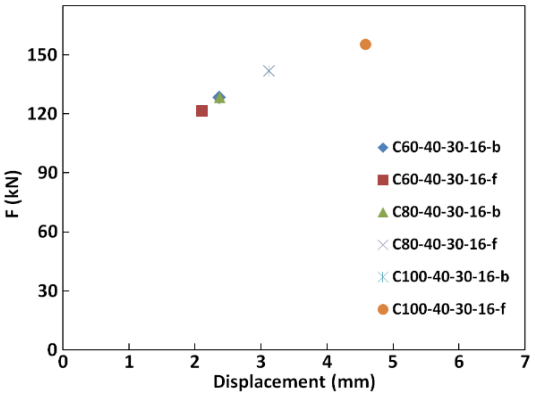


(b) Crack initiation load point

Fig. 16 Composite beam with different channels in face to face and back to back arrangements ($f_c$ = 30 MPa)

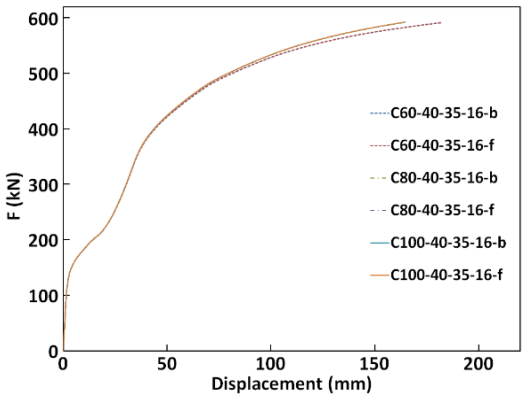


(a) Force-displacement diagram

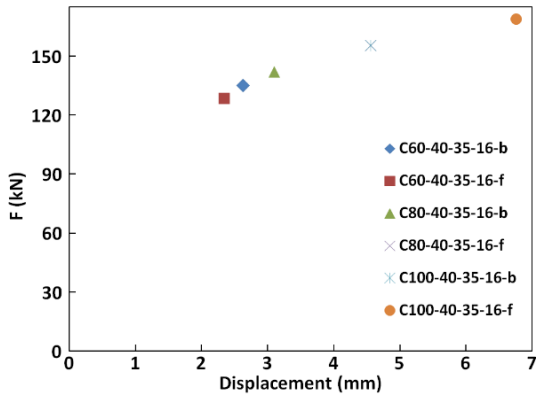


(b) Crack initiation load point

Fig. 17 Composite beam with different channels in face to face and back to back arrangements ($f_c$ = 35 MPa)

crack initiation load rises significantly with increasing size of channels. In all of these cases, plastic strain was formed later in the concrete in face to face arrangement compared to that of back to back.

### 3.4 The effects of the length and spacing of channels

Force-displacement diagrams of composite beams were plotted for face to face and back to back arrangements of UNP60 channels. 16 channels of 4 cm length, 16 of 8 cm length and 8 of 8 cm length were used for the concrete of 25, 30 and 35 MPa compressive strengths. The curves are shown in Figs. 18 to 20.

In all models, the crack initiation load rises with increasing length of channel; moreover, the crack initiation load is more with increasing number of channels. Concerning the 16 channels of

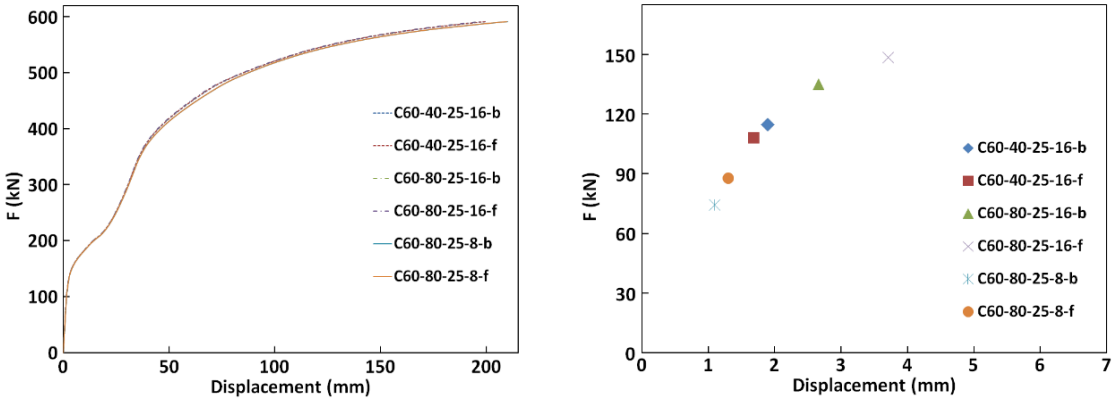


(a) Force-displacement diagram (b) Crack initiation load point

Fig. 18 Composite beam with different numbers, lengths and arrangements of channels ($f_c$ = 25 MPa)

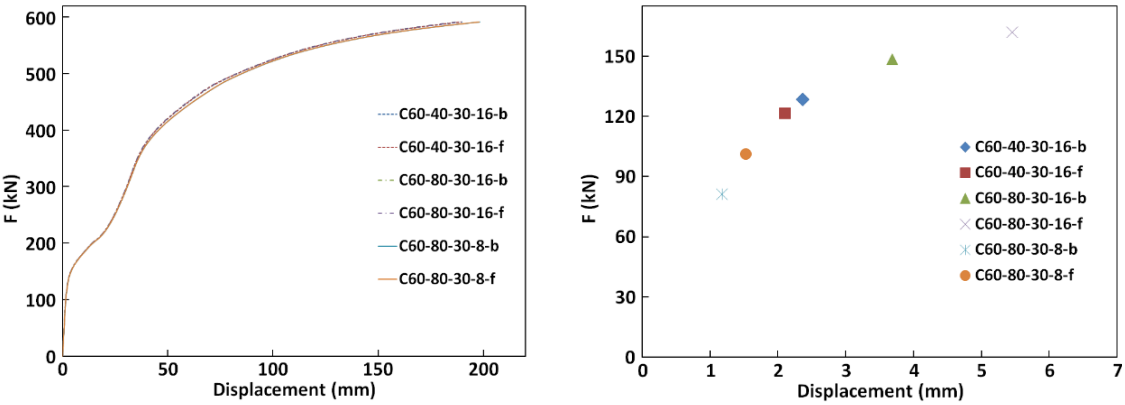


(a) Force-displacement diagram (b) Crack initiation load point

Fig. 19 Composite beam with different numbers, lengths and arrangements of channels ($f_c$ = 30 MPa)

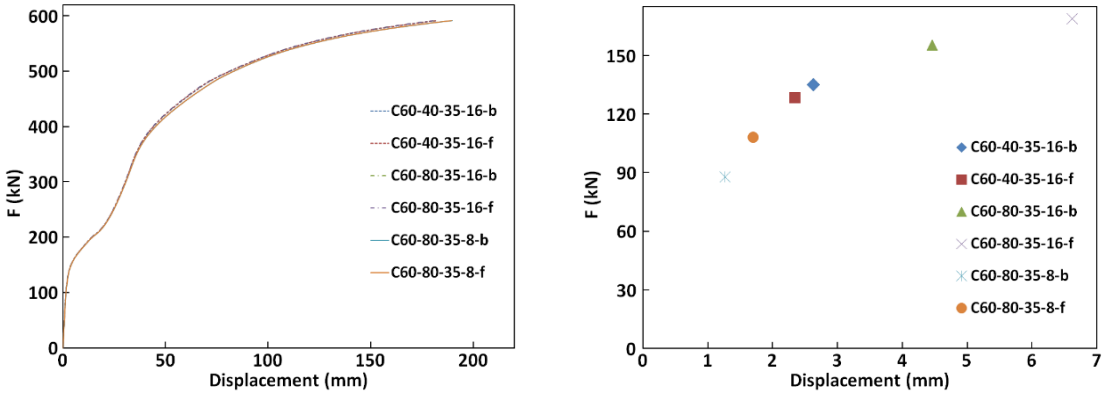


(a) Force-displacement diagram (b) Crack initiation load point

Fig. 20 Composite beam with different numbers, lengths and arrangements of channels ($f_c$ = 35 MPa)

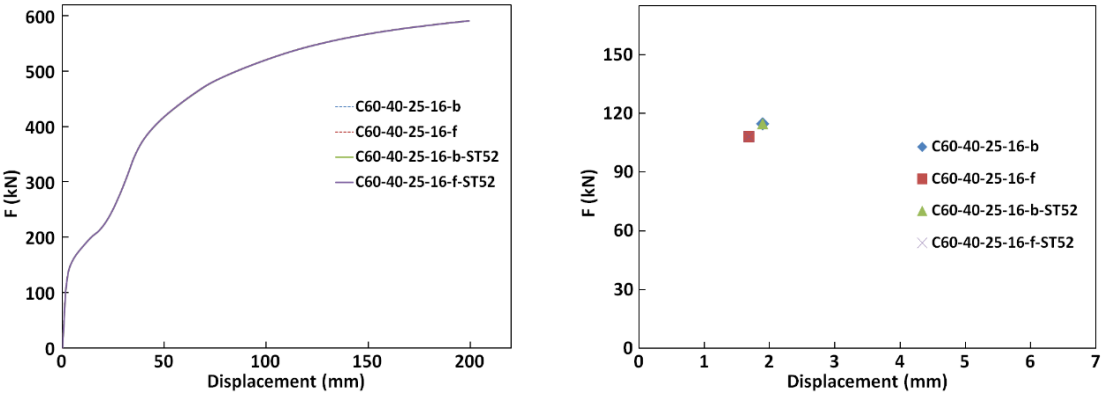


(a) Force-displacement diagram (b) Crack initiation load point

Fig. 21 Composite beam with different steel types of channels ($f_c$ = 25 MPa)

4 cm length, the crack initiation load is more compared to the 8 channels of 8 cm length. According to 'b' in Figs. 18 to 20, the plastic strain in the concrete is formed later in the face to face arrangement, compared to that of back to back in all of the specimens.

### *3.5 The effect of steel type of channel*

The results obtained by applying ST52 and ST37 steel types for channel shear connectors as the channels, have the same trend. Considering the compressive strength of 25 MPa for concrete, the force-displacement diagram was plotted for channels with the above mentioned steel types and shown in Fig. 21(a). Force-displacement diagrams as well as the results of back to back and face to face channel shear connectors are all the same for these steel types.

Considering Fig. 21(b), the crack initiation load points are similar in the specimens with channel steel grades of ST52 and ST37.

## 4. Conclusions

Finite element analyses were conducted to study the differences between face to face and back to back arrangements of channel shear connectors, obtain force-displacement diagram of composite beam and calculate the crack initiation load. The results derived from the performed analyses are briefly summarized as follows:

- By increasing the compressive strength of concrete for a particular size of channel, the obtained force-displacement diagrams are the same in the two arrangements of the channels, face to face and back to back. Crack initiation load rises with increasing channel size, number and length of channels.
- The crack initiation load is more with 16 channels of 4 cm length compared to those with 8 channels and 8 cm length. The crack initiation load points are quite similar in the back to back and face to face arrangements concerning the specimens with the channel of UNP60 and 4 cm length for different concrete compressive strengths. However, the crack initiation load is more in the face to face arrangement compared to that of back to back for different concrete compressive strengths in the specimens with channels of UNP80, UNP100 and UNP60 with 8 cm length. Changing the steel grade of channels has no effect on the result.
- According to the conducted analyses, it can be concluded that there is no significant difference between the two arrangements of face to face and back to back. However, face to face arrangement shows a little better performance in comparison to back to back concerning the crack initiation load.

## References

Abe, H. and Hosaka, T. (2002), "Flexible shear connectors for railway composite girder bridge", *ASCE Compos. Construct. Steel Concrete IV*, 71-80.

AISC (2010), Specification for Structural Steel Buildings, American Institute of Steel Construction; Chicago, IL, USA.

Baran, E. and Topkaya, C. (2012), "An experimental study on channel type shear connectors", *J. Construct. Steel Res.*, **74**, 108-117.

Baran, E. and Topkaya, C. (2014), "Behavior of steel-concrete partially composite beams with channel type shear connectors", *J. Construct. Steel Res.*, **97**, 69-78.

Brendel, G. (1964), "Strength of the compression slab of T-beams subject to simple bending", *ACI J. Proceedings*, **61**(3), 57-76.

Chung, K.F. and Chan, C.K. (2011), "Advanced finite element modeling of composite beams with high strength materials and deformable shear connectors", *Procedia Eng.*, **14**, 1114-1122.

Code, C.-F.M. (1990), *Model Code for Concrete Structures*, Bulletin d'Information, (117-E).

Hibbitt, D., Karlsson, B. and Sorenson, P. (2011), *Simulia ABAQUS 6.11 Users' Manual*.

Lubliner, J., Oliver, J., Oller, S. and Oñate, E. (1989), "A plastic-damage model for concrete", *Int. J. Solid. Struct.*, **25**(3), 299-326.

Maleki, S. and Bagheri, S. (2008a), "Behavior of channel shear connectors, Part I: Experimental study", *J. Construct. Steel Res.*, **64**(12), 1333-1340.

Maleki, S. and Bagheri, S. (2008b), "Behavior of channel shear connectors, Part II: Analytical study", *J. Construct. Steel Res.*, **64**(12), 1341-1348.

Maleki, S. and Mahoutian, M. (2009), "Experimental and analytical study on channel shear connectors in fiber-reinforced concrete", *J. Construct. Steel Res.*, **65**(8-9), 1787-1793.

Nguyen, Q.H., Hjiaj, M., Uy, B. and Guezouli, S. (2009), "Analysis of composite beams in the hogging

moment regions using a mixed finite element formulation", *J. Construct. Steel Res.*, **65**(3), 737-748.
Pashan, A. (2006), "Behavior of channel shear connectors: Push-out tests", M.Sc. Thesis; University of Saskatchewan, Saskatoon, SK, Canada.
Salmon, C.G. and Johnson, J.E. (1996), *Steel Structure*: *Design and Behavior*, University of Wisconsin, Madison, WI, USA.
Shariati, M., RamliSulong, N.H. and Arabnejad Khanouki, M.M. (2012), "Experimental assessment of channel shear connectors under monotonic and fully reversed cyclic loading in high strength concrete", *Mater. Des.*, **34**, 325-331.
Shariati, M., RamliSulong, N.H., Suhatril, M., Shariati, A., Arabnejad Khanouki, M.M. and Sinaei, H. (2013), "Comparison of behavior between channel and angle shear connectors under monotonic and fully reversed cyclic loading", *Construct. Build. Mater.*, **38**, 582-593.
Vasdravellis, G., Uy, B., Tan, E.L. and Kirkland, B. (2012), "The effects of axial tension on the hogging-moment regions of composite beams", *J. Construct. Steel Res.*, **68**(1), 20-33.
Viest, I.M. (1974), "Composite steel-concrete construction", *ASCE J. Struct. Div.*, **100**(5), 1085-1139.

*CC*